XA9949524

"BULK MOISTURE DETERMINATION IN BUILDING MATERIALS BY FAST NEUTRON / GAMMA TECHNIQUE".

IVAN PADRON DIAZ, LUIS FELIPE DESDIN, GUIDO MARTIN HERNANDEZ, KATHERIN SHTEJER, NAIPY PEREZ TAMAYO, CESAR CEBALLOS, OLGA LEMUS.

Centro de Estudios Aplicados al Desarrollo Nuclear (CEADEN), Street 30 No.502. Miramar, La Havana, Cuba.

1. FAST NEUTRON/ GAMMA TRANSMISSION IMPROVEMENTS.

1.1 . NE-213 scintillation pulse shape discrimination approach.

❖ **Designing, construction and testing of the pulse shape discrimination system.**
In organic scintillators, like stilbene and NE-213, the γ-rays produce recoil electrons, while the neutrons produce recoil protons. Assuming equal recoil energies for protons and electrons, the photomultiplier output shows similar signal front but different fall time signal. In this case, the current signal form is determined by the interaction of two (fast and slow) components [1]:

$$I_a(A) = \{\frac{A_r}{\tau_r}\exp(-\frac{\tau_r}{t}) + \frac{A_s}{\tau_s}\exp(-\frac{\tau_s}{t})\}.\ I_{m\ ax}$$

Where: τ_r - fast fall time constant (similar for all types of particle)

τ_S - slow fall time constant

A_r , A_s - fast and slow fractions of the total current amplitude.

When the pulses are integrated and differentiated by two differentiating networks, the cross over point can be used to identify neutrons and γ-rays pulses.
In order to improve the fast neutron/gamma discrimination in the transmission system employing the NE-213 scintillation detector a pulse shape discrimination system was constructed at the CEADEN.

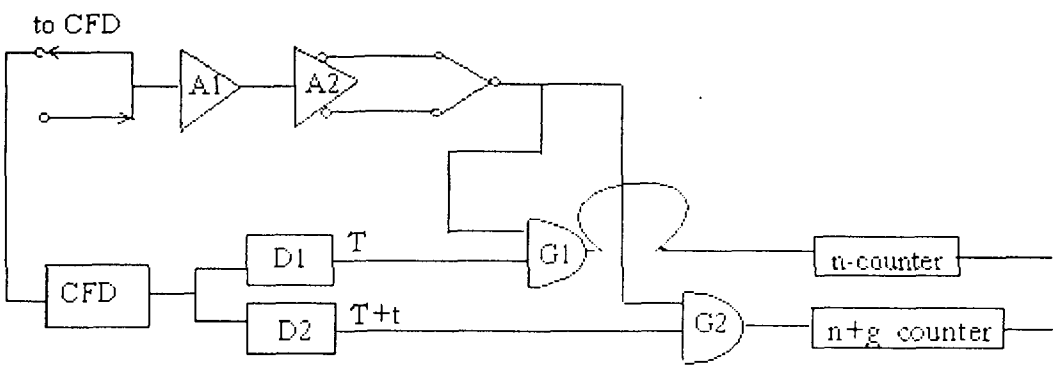

Fig. 1. Block diagram of the circuit.

The anode pulse of the photomultiplier is integrated and differentiated in a preamplifier A1. After that the shaped signal is then fed to a high-gain limiting amplifier A2. The separation of the zero-crossing points corresponding to gammas or neutrons is now greatly enhanced. The overlaps of the amplifier signal and the strobe pulses are formed in the gates G1 and G2. In our set-up the strobe signal is triggered by the output pulse of a constant fraction discriminator CFD, which is delayed and stretched in D1 and D2.

- Time resolution characterisation of the pulse shape discrimination system using a (dia.40x30)mm NE-213 scintillation detector [2].

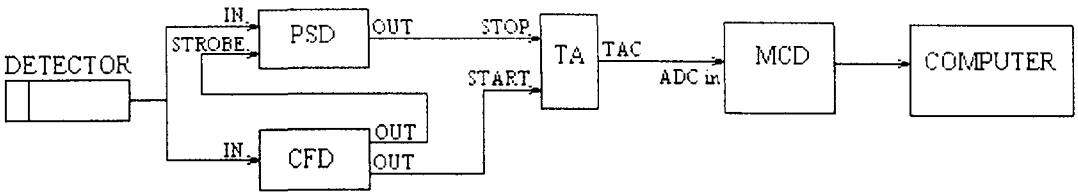

Fig. 2. Electronic scheme for time resolution measurement.

PSD – Pulse shape discriminator (Made in CEADEN)
CFD – Constant fraction discriminator (Canberra, model 1428)
TA – Time analyser (Canberra, model 2043).
MCD/PC – Multichannel data processor.
ADC – Analog-digital converter (FAST, model 7070).

$$\Delta t_{channel} = \frac{\text{time range}}{ADC gain} = \frac{500 nseg}{8192 channels} = 0.061 nseg/channel$$

$$\text{Time resolution} = \Delta t_{channel} \cdot \text{FWHM} = 0.4 \text{ nseg.}$$

- **Modelling the fast neutron and gamma interactions by Monte Carlo simulation method with the material samples to be measured.**

  In order to have a good knowledge of the neutron detecting efficiency and its energy dependence 2 Monte Carlo simulation codes have been developed in our laboratory:

  - Neutron detection efficiency calculation in NE-213 scintillation detector for low energy threshold.

    Several improvements have been made to the Monte Carlo neutron efficiency code of Stanton-Cecil [3, 4] to provide improved agreement with experimental measurements in the energy range up to 20 MeV and at low energy thresholds. The improvements include the adoption of a new method for the detector resolution simulation, readjustment of the cross sections according to the last reported evaluations, consideration of the light attenuation in the scintillator and neutron/gamma discrimination correction.

    The code also includes some new light response functions to improve calculation for proton energy less than 2 MeV. The calculations show good agreement with reported measurements.

- NE-213 detector calibration using radio-isotopic gamma sources and Monte Carlo simulation method.
  Some gamma spectra were measured using a (2'' dia. x 2'') NE-213 liquid scintillation detector and an EMI-9880 low noise photomultiplier.
  The response function is calculated considering the Compton scattering in the scintillator, the escape of electrons, the γ-rays multiscattering and the effect of finite resolution of our detection system.

  Comparing the measured and calculated response functions is possible to determine the position of the Compton edge [5].

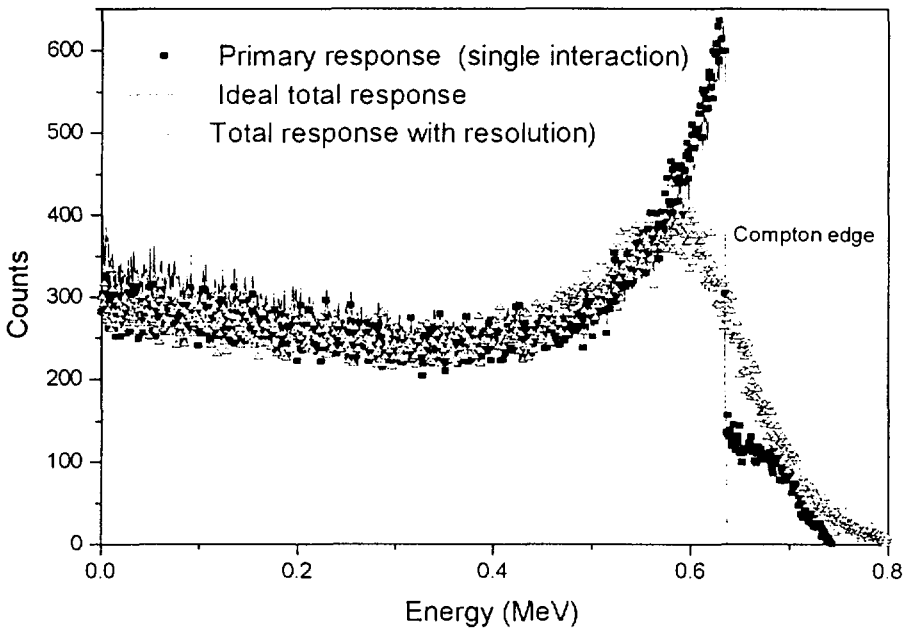

Fig. 3 NE-213 detector simulated response function for gamma radiation.

1.2. Separate neutron / gamma detection approach.

1.2.1. Measuring by fast neutron technique the moisture content in building material samples.

Obviously, the most efficient fast neutron detector is an organic scintillator utilising electronic pulse shape discrimination. However, it has the disadvantage of requiring highly complex electronics to achieve count rate stabilities better than 0.5% relative [6].

In our project we decided to replace the NE-213 detector by separate neutron and gamma detectors. As neutron detector we will use a BF_3 tube surrounded by 100mm thickness of paraffin and a collimated (dia.56 mm) NaI(Tl) located above the paraffin as the gamma detector.

For this reason, a preliminary study of fast neutron and gamma transmission methods have been carried out by separate utilising different concrete blocks usually employed for biological shielding designs.

The block dimensions are (300x300x50) mm and were made of lead, paraffin, and some types of concrete (barite, limestone, serpentine, magnetite and limonite). The water was measured in a brass container with the same geometry.

Table No.1: Composition of concrete blocks.

Concrete type	Density	Basic Content (%)	H_2O content (%)
Barite	3.83	$BaSO_4$ (50%) Al_2O_3 (2%)	2.91
Limestone	2.63	$CaCO_3$	---
Serpentine	2.75	SiO_2 (40%) MgO (35%)	12.99
Magnetite	3.88	Fe_2O_3 (72%) FeO (6%)	9.3
Limonite	2.92	Fe_2O_3 (47%) SiO_2 (2%)	9.84

1.2.2. Neutron transmission measurements using an Am-Be neutron source and a BF_3 detector (long counter geometry).

The neutron transmission coefficient is defined as $\mathbf{T(x) = (I(x) - I_f) / (I_0 - I_f)}$, where $\mathbf{I_0}$ is the count speed without sample, $\mathbf{I(x)}$ is the count speed with **x** thickness sample and $\mathbf{I_f}$ is the background due to the neutron reflection on the walls.

For our geometry the factor $\mathbf{R = I_0 / I_f} = 2.58 \pm 0.01$ don't depends of the sample material. In our concrete blocks the %w of hydrogen is greater than 0.1%, that so, the λ_{rel} is greater than diffusion length for thermal neutrons and, for this reason, the accumulation factor contribution to the flux variation for low energy neutrons can be considered less important than for fast neutrons. Though the long counter is sensible to neutrons of all energies, the decisive role belong to fast neutrons, specifically to 6-8 MeV neutrons.

1.2.3. Density and homogeneity determination by gamma transmission method using a collimated ^{137}Cs source ($A=3.7x10^8$ Bq).

Table No.2: Concrete blocks characteristics.

Concrete	μ	$\Delta\mu$	$\Delta\mu / \mu$	λ (cm)	Ω (cm)	I/I_0 (%)	ρ
Barite	0.262	0.004	0.015	3.8	4.5	26.9	3.83
Limestone	1.161	0.002	0.012	6.2	7.3	44.5	2.63
Serpentine	0.155	0.007	0.045	6.5	7.6	46.1	2.75
Magnetite	0.221	0.004	0.018	4.5	5.3	33.1	3.88
Limonite	0.184	0.006	0.033	5.4	7.6	39.9	2.92

The parameters are μ : lineal attenuation coefficient for gamma rays, $\Delta\mu$: experimental dispersion of μ, λ : relaxation coefficient for gamma rays, Ω : thickness necessary for an attenuation equivalent to 1 cm of lead, $\mathbf{I/I_0}$: count speed rate for 5 cm thickness and $\rho[g/cm^3]$: material density.

2. Establishment and determination of the neutron generator parameters related to the neutron production (flux, energy spread, and angular distribution).

- Ion beam current calibration at the associated particle target head using a current integrator. (This work began during the Prof. Julius G. Csikai expert mission).
- Design and construction of a heavy water hydrolysing system for the deuterium gas production [7].

3. Neutron reflection experiments.

In addition to our work plan for the first year some experiments have been done in neutron reflection (related to CRP Area 2.1) in order to compare the sensitivity and practical possibilities of transmission and reflection methods. A "open geometry" neutron reflection system was designed by Prof. J. Csikai during his expert mission in our laboratory.

In order to check the total counting system (detector + electronic devices), we measured the well-known dependence of the excess count rate (η) relating to the thickness of material (water in this case). It was obtained just the same saturation curve you obtained before. (The measurement time was t=20 min for each point).

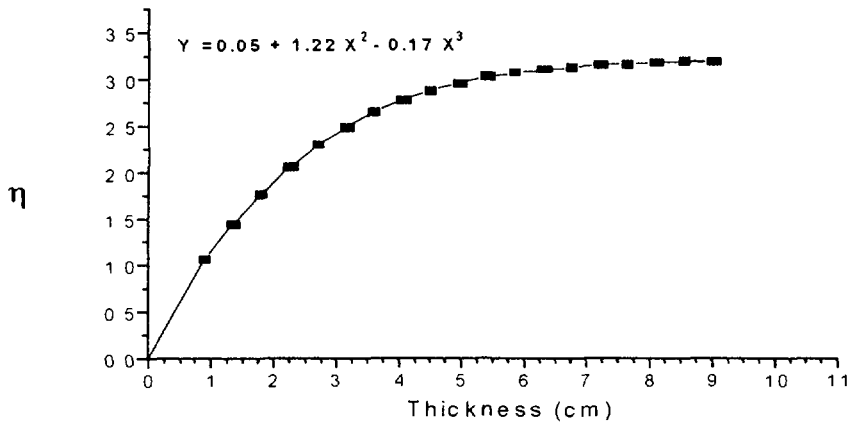

Fig. 4 Excess count rate dependence of the material thickness.

Finally, we carried out both: the measurement and the simulation (MCNP) of the behaviour of the excess count rate vs. H (w%) for some pure hydrocarbons and alcohols. Both were plotted and in each case the result was the expected linear relationship between η and H (w%). In the case of MCNP calculations, we have been varying different parameters (mainly geometric ones) in order to improve the calculation results.

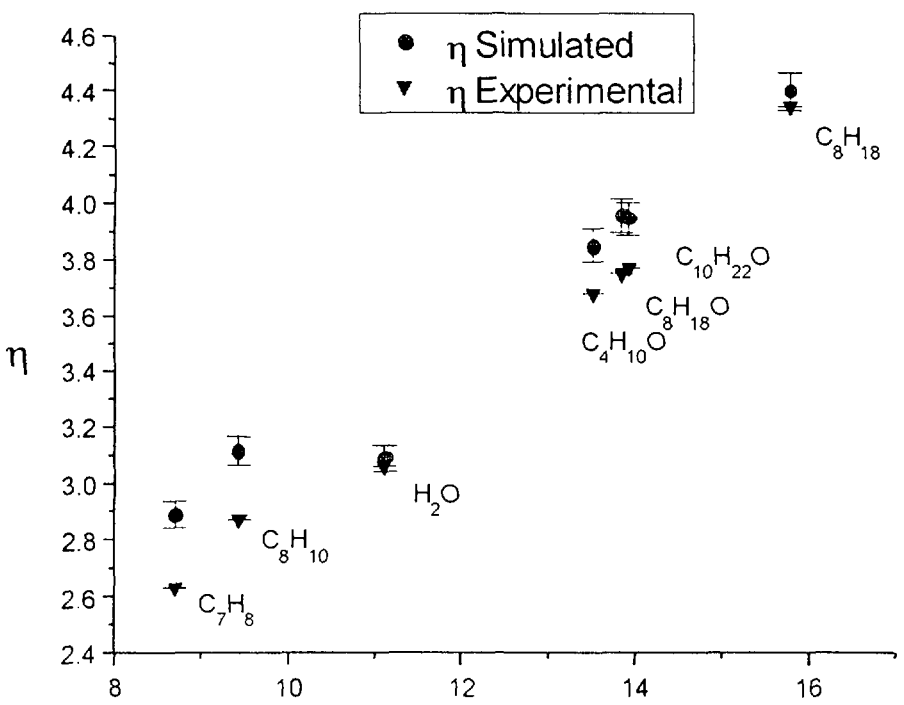

Fig.5 Behaviour of the excess count rate vs. H (w%) for some pure hydrocarbons and alcohols

A study of neutron reflection coefficients for some metals was realised using this system. Adding polyethylene foils to the metals samples the hydrogen content and its homogeneity was estimated.

4. Other works related to the CRP topics.

In order to study the microscopic behaviour of hydrogen (related to CRP Area 2.4) in 27 different samples a holder, fixed to the neutron generator rotating target, was designed by Prof. J. Csikai and constructed at the CEADEN. This experimental study of ion implantation and deuterium diffusion coefficient in metals will be carried out using activation analysis and associated particle method.

- In collaboration with Prof. Csikai some calculations using neutron transport codes have been carried out and the results should be published in the article:

L. Olah, A. Fenyvesi, J. Jordanova, A. M. El-Megrab, A. D. Majdeddin, Darsono, N. Pérez, Yousif Ali and J. Csikai.

" Measurements and calculations of neutron leakage spectra from slabs irradiated with $^{9}Be(d,n)^{10}B$, $^{2}H(d,n)^{3}He$ and Pu-Be neutrons".

Paper has been submitted for publication in JARI.

REFERENCES

[1] A.P. Tsitovich "Nuclear radioelectronic", Moscow (1967).
[2] T.G.Miller in Nuclear Instruments and Methods" 63, (1968), p. 121.
[3] R.A. Cecil in Nuclear Instruments and Methods" 161, (1979), p. 439.
[4] N.R. Stanton in COO-1545-92, February 1971.
[5] G. Dietze, H. Klein in Nuclear Instruments and Methods" 193, (1982), p. 549.
[6] B.D. Sowerby, M.J. Millen and P.T. Rafter in Nucl. Geophys. Vol.2, No.1 (1988)
[7] J. Csikai et al. IAEA-TECDOC-913, November 1996.